Heat Transfer Characteristics of Porous Rocks

DAIZO KUNII and J. M. SMITH

Northwestern University, Evanston, Illinois

Equations are derived for predicting the effective thermal conductivity of beds of unconsolidated particles containing stagnant fluid. The effective thermal conductivity at these conditions, called the stagnant conductivity, is a function of the thermal conductivities of the solid and fluid phases, the void fraction, and, if radiation is important, the emissivity, mean temperature, and diameter of the solid particles. Comparison with the available experimental data indicates that the equations are satisfactory for fluids and solid particles of both high and low thermal conductivities.

To extend the theory to beds of consolidated particles, it is supposed that consolidated beds are formed by partial clogging and cementing of beds of unconsolidated particles. With this assumption the theoretical equations for packed beds are extended to include such materials as sandstone and porous metals. The resulting expressions for the stagnant conductivity involve a consolidation parameter characteristic of the solid material. This quantity accounts for the heat transfer across the contact surfaces between cemented or clogged particles. The equations correctly predict the effect of void fraction and solid and fluid thermal conductivities on the heat transfer properties of sandstones and sintered metal systems.

The heat transfer characteristics of fluid-bearing rocks are of growing importance as a result of the significance of thermal methods of petroleum production. The successful design and evaluation of these methods depends directly upon heat transfer rates in porous rocks containing stationary and flowing fluid. There have been several experimental investigations of temperature gradients in porous media filled with stationary fluid, but essentially no data have been published for the moving fluid case. Also there is a need for an adequate theory to explain heat transfer rates in consolidated media for both static and flowing fluid conditions. In contrast, the thermal characteristics of packed beds of larger sized unconsolidated particles, for example fixed-bed catalytic reactors, have been studied intensively.

This investigation is a theoretical study of effective thermal conductivities of porous media filled with stationary fluid, that is stagnant conductivities. The results are applied to beds of both unconsolidated particles and consolidated materials such as sandstone. Later studies will be concerned with heat transfer perpendicular and parallel to the direction of flowing fluid.

PREVIOUS WORK

Stagnant conductivities of porous sandstones have been measured experimentally by several observers (*2, 3, 7, 27, 50*), but few attempts have been made to explain the results in terms of physical properties such as the thermal conductivities of the solid and fluid phases and the void fraction.

In packed beds of unconsolidated particles the major experimental studies of stagnant conductivities are summarized in references *16, 19, 20, 21, 29, 40, 42, 45* and the theoretical studies in references *8, 13, 36, 38, 41, 44*. Yagi and Kunii (*45*) specifically considered the heat transfer mechanism through the fluid film near the contact surfaces, or points.

Effective thermal conductivities in packed beds with flowing fluids have been studied by a number of investigators (*1, 4, 5, 6, 9, 11, 17, 18, 21, 22, 24, 25, 26, 28, 30, 31, 35, 37, 39, 43, 46, 47, 48,* and *49*).

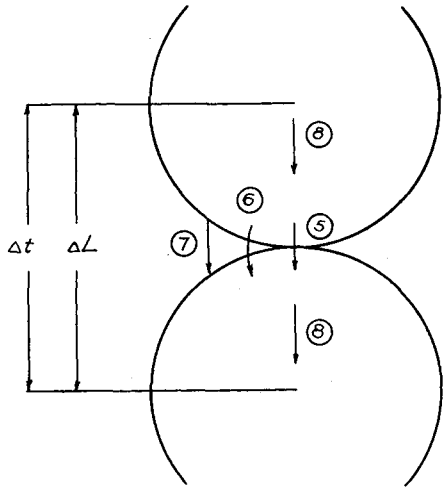

Fig. 1. Heat transfer model for packed bed of unconsolidated particles.

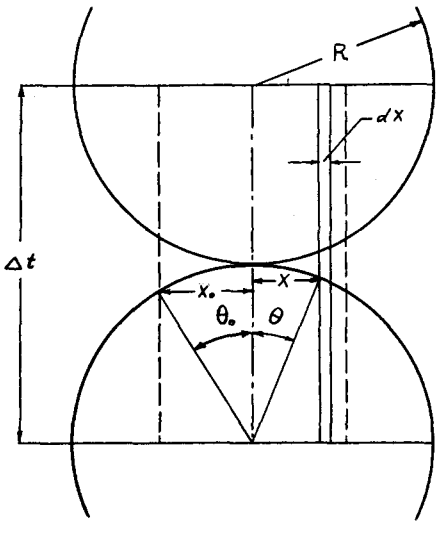

Fig. 2. Model for heat transfer near contact points of particles.

From these data approximate values of the stagnant conductivity can be obtained by extrapolation to zero flow rate.

Previous theoretical investigations of heat transfer in consolidated materials have been directed toward the refractory industry (*10, 23, 32*). Francl and Kingery (*12*) measured the effect of void fraction of a continuous solid phase with isolated small pores of air and found that the stagnant conductivity could be represented by

$$k_e^\circ/k_s = 1-\epsilon' \text{ (below 900°F.)} \qquad (1)$$

RELATIONSHIP BETWEEN PACKED BEDS AND CONSOLIDATED POROUS ROCKS

The effect of void fraction on the stagnant conductivity of consolidated porous media like sandstone is different from its effect on refractory materials. The decrease in conductivity with increasing void fraction is observed to be concave downward rather than linearly.

There are some indications that consolidated porous rocks such as sandstone are more closely related to packed beds of unconsolidated particles than to refractory materials. It is conceivable, for example, that underground sandstones were formed by consolidation of loose materials. Accordingly, it appears reasonable to analyze the heat transfer problem by first considering the behavior of beds of unconsolidated particles.

MECHANISM OF HEAT TRANSFER IN BEDS OF UNCONSOLIDATED PARTICLES

Figure 1 shows a cross section of two spherical particles in contact with each other. It is presumed that the particles are surrounded by stagnant fluid. Heat transfer is assumed to occur in the vertical direction by the following mechanisms:

1. Heat transfer through the fluid in the void space by conduction and by radiation between adjacent voids (when the voids are assumed to contain a nonabsorbing gas).
2. Heat transfer through the solid phase.
   a. Heat transfer through the contact surface of the solid particles.
   b. Conduction through the stagnant fluid near the contact surface.

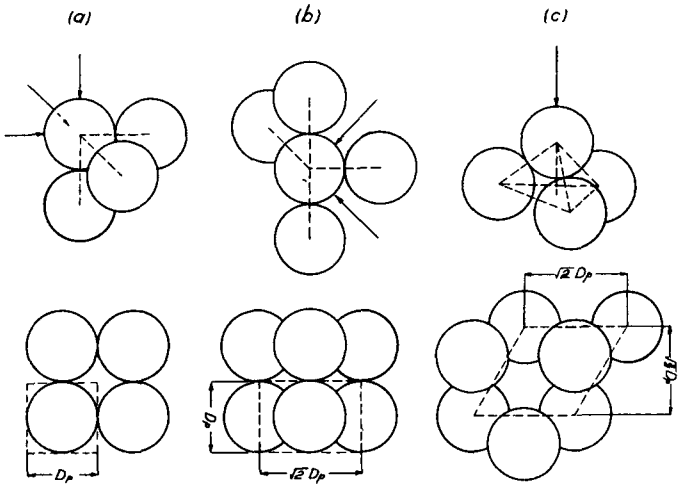

Fig. 3. Heat transfer directions for loose packing of spheres.

c. Radiation between surfaces of solid (when the voids are assumed to contain a nonabsorbing gas).
d. Conduction through the solid phase.

Over-all mechanisms 1 and 2 are in parallel with each other. Mechanism *d* is in series with the combined result of parallel mechanisms *a*, *b*, and *c*. This model is somewhat similar to that proposed by Yagi and Kunii (45). Mechanism *a* will be interpreted in terms of a heat transfer coefficient for convenient application to consolidated porous media such as sandstone.

According to the model in Figure 1, the effective thermal conductivity is given by $-k_e^\circ(\Delta t)/(\Delta L)$ = [heat flux in void space (mechanism 1)] + [heat flux through solid phase (mechanism 2)].

Therefore

$$\text{(mechanism 1)} \qquad -k_e^\circ \frac{\Delta t}{\Delta L} = -k_g \epsilon \frac{\Delta t}{\Delta L} + h_{rv}\,\epsilon\,(-\Delta t) \qquad \text{(mechanism 2)} \qquad + q_s \tag{2}$$

On the other hand the temperature drop in the particle = (temperature drop in solid phase) + (temperature drop near the contact surface), or

$$\Delta t = \Delta t_s + \Delta t_{gs} \tag{3}$$

The individual temperature drops may be written in terms of the heat flux in the solid phase:

$$\Delta t_s = \frac{-q_s}{\left(\frac{k_s}{l_s}\right)} \frac{1}{1-\epsilon} \tag{4}$$

$$\Delta t_{gs} = \frac{-q_s}{\frac{k_g}{l_v} + h_p + h_{rs}} \frac{1}{1-\epsilon} \tag{5}$$

In these expresssion l_s is the thickness of a slab of solid material which would offer the same resistance to heat transfer as the spherically shaped particle; l_v is the thickness of a slab of stationary fluid which would offer the same heat transfer resistance as the filaments of fluid near the contact point between particles.

Combination of Equations (2) through (5) results in the following expression for k_e°:

$$k_e^\circ = \epsilon[k_g + h_{rv} \cdot \Delta L] + \frac{(1-\epsilon)\,\Delta L}{\frac{1}{\frac{k_g}{l_v} + h_p + h_{rs}} + \frac{l_s}{k_s}} \tag{6}$$

which may be written

$$\frac{k_e^\circ}{k_g} = \epsilon\left[1 + \beta\frac{h_{rv} \cdot D_p}{k_g}\right] + \frac{\beta(1-\epsilon)}{\frac{1}{\frac{1}{\phi} + \frac{D_p}{k_g}(h_p + h_{rs})} + \gamma\left(\frac{k_g}{k_s}\right)} \tag{7}$$

This general equation may be simplified in many instances. For example, except at very low pressures the term for heat transfer through the contact surfaces (mechanism *a*) can be neglected. Then

$$\frac{k_e^\circ}{k_g} = \epsilon\left[1 + \beta\frac{h_{rv} \cdot D_p}{k_g}\right] + \frac{\beta(1-\epsilon)}{\frac{1}{\frac{1}{\phi} + \frac{D_p \cdot h_{rs}}{k_g}} + \gamma\left(\frac{k_g}{k_s}\right)} \tag{8}$$

When the void spaces contain liquid instead of gas, the contributions due to radiant heat transfer disappear:

$$\frac{k_e^\circ}{k_g} = \epsilon + \frac{\beta(1-\epsilon)}{\phi + \gamma\left(\frac{k_g}{k_s}\right)} \tag{9}$$

Even for gaseous systems the radiation contributions are negligible, except for relatively large particles and high temperature (above 900°F.). The radiation coefficients, when necessary, may be estimated by the equations proposed by Yagi and Kunii (45).

To use Equations (7) to (9), it is necessary to know the numerical values of the three quantities β, γ, ϕ. For close packing of spheres, as shown in Figure 4, the average value of β is

$$\beta = \frac{1}{D_p}\frac{1}{3}\left[\left(\frac{2}{3}\right)^{1/2} + 1 + \left(\frac{3}{2}\right)^{1/2}\right] D_p = 0.895$$

For the most loose or open packing, β should be unity. Therefore its value will range from 0.9 to 1 for almost all actual packed beds. The value of γ depends upon l_s; it will be assumed to be the length of a cylinder having the same volume as the spherical particle; that is

$$l_s = \left(\frac{\pi}{6}D_p^3\right) \Big/ \left(\frac{\pi}{4}D_p^2\right) = \frac{2}{3}D_p$$

$$\gamma = l_s/D_p = \frac{2}{3}$$

The most difficult quantity to evaluate is ϕ, which is a measure of the effective thickness l_v of the fluid film adjacent to the contact surface of two solid particles. It is determined theoretically in the next section.

HEAT TRANSFER THROUGH THE FLUID PHASE NEAR THE CONTACT SURFACE OF SOLID PARTICLES

Heat transfer through the fluid filaments adjacent to the solid particles may be analyzed by reference to Figure 2. Even though but one contact point is shown, each particle will have several contact points on its semispherical surface which contribute to the heat transfer in one direction. One should consider the general case and assume that the fraction $(1/n)$ of the total heat flux passes through the fluid film near one contact point. The second assumption is that the heat flow is parallel to the axis between the particles. Then the fraction of the total heat transfer associated with one contact point is

$$\frac{1}{n} = \frac{\pi x_o^2}{\pi R^2} = \sin^2\theta_o \tag{10}$$

With these concepts the following expression can be derived for q:

$$q = \int_0^{q_o} dq = \pi R\, k_g\, \Delta t \left(-\frac{\kappa}{\kappa-1}\right)^2 \left[\ln\{\kappa-(\kappa-1)\cos\theta_o\} - \frac{\kappa-1}{\kappa}(1-\cos\theta_o)\right] \tag{11}$$

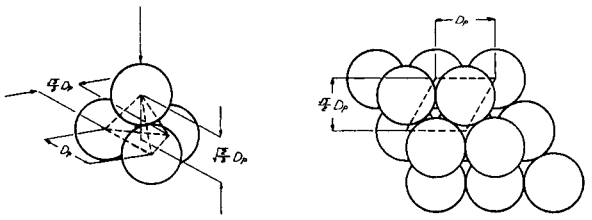

Fig. 4. Directions of heat transfer for close packing of spheres.

where κ is k_s/k_g.

Equation (11) includes the heat transfer through the solid phase in series with the filaments of fluid. Hence q can be expressed in terms of the sum of the resistances of the two steps; that is

$$q = \frac{\pi(R \sin\theta_o)^2 \Delta t}{\frac{2R\left(\frac{2}{3}\right)}{k_s} + \frac{l_v}{k_g}} \qquad (12)$$

where $2R(2/3) = \gamma D_p = l_s$ and is therefore the effective length of the spherical solid for thermal conduction.

Employing the definition of l_v in terms of ϕ and noting that $D_p = 2R$, one can combine Equations (11) and (12) to give

$$\phi = \frac{1}{2} \frac{\left(\frac{\kappa-1}{\kappa}\right)^2 \sin^2\theta_o}{l_n\{\kappa-(\kappa-1)\cos\theta_o\} - \frac{\kappa-1}{\kappa}(1-\cos\theta_o)} \qquad (13)$$

where $\kappa = k_s/k_g$, and $\sin^2\theta_o = 1/n$.

Equation (13) is the basic expression for ϕ for a single contact point (Figure 2). To obtain the required ϕ for use in Equations (7) to (9), the number of contact points on a surface of one half of a single particle must be determined.

To estimate n, two arrangements of particles, state 1 for the most open packing and state 2 for close packing, should be considered. For state 1, composed of spherical particles of uniform size packed with their centers at the corners of cubes, three axes of symmetry (a), (b), and (c) must be considered, with the directions of heat transfer as shown in Figure 3. Orientations (b) and (c) have two and three contact points, respectively. However these numbers must be corrected for the cross-sectional areas perpendicular to the directions of heat transfer and for the frequency of the orientations. From geometrical considerations one can show that the data for each orientation are

Orientation	(a)	(b)	(c)
Contact point	1	2	3
Area corresponding to one particle	D_p^2	$\sqrt{2}D_p^2$	$\sqrt{3}D_p^2$
Number of directions	3	2	4

The derivation of Equation (13) is based upon orientation (a), as shown in Figure 2. Hence the equivalent number of contact points for orientation (b) for use in connection with Equation (13) will be n'_1, given by the expression

$$n'_1 = (2)\frac{D_p^2}{(\sqrt{2}\,D_p^2)}\left(\frac{2}{3}\right) = 0.945$$

In this manner the average number of

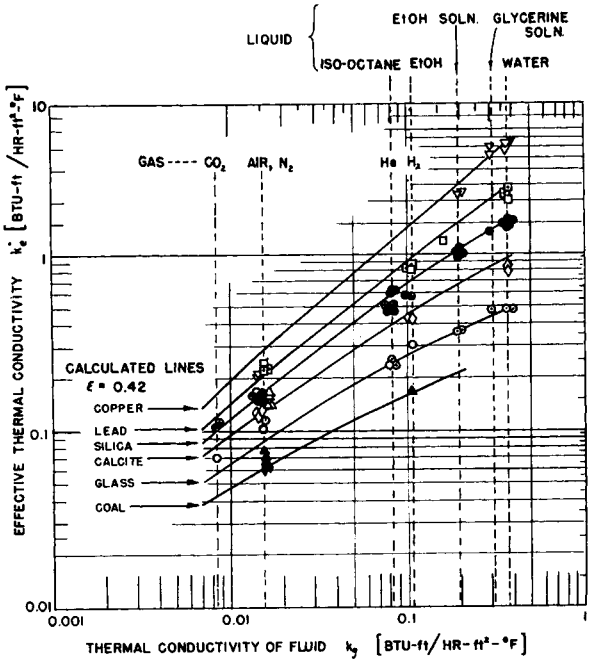

Fig. 6. Comparison of calculated and experimental data, unconsolidated particles.

TABLE 1—KEY FOR FIGURE 6

Symbol	Solid	Av. diam. (in.)	Void fraction	Observers	Ref.
▲	coal	–	0.437	Schumann and Voss	(36)
◆	coal	–	0.40	Saito and Okagaki	(33)
○	glass	0.0212	–	Weiniger and Schneider	(42)
⊙	glass	0.0132-0.089	0.408-0.431	Preston	(29)
△	calcite	0.098-0.563	0.458-0.493	Waddams	(40)
◇	calcite	0.056-0.112	0.447-0.465	Kimura	(20)
●	silica	0.00504-0.0960	0.408-0.439	Preston	(29)
⊕	alumina	0.0189-0.0429	0.432-0.461	Weiniger and Schneider	(42)
□	lead	0.103	0.40	Schumann and Voss	(36)
▣	lead	0.0132-0.0179	0.397-0.420	Kimura	(20)
▽	copper	0.0059-0.0068	0.384-0.392	Preston	(29)

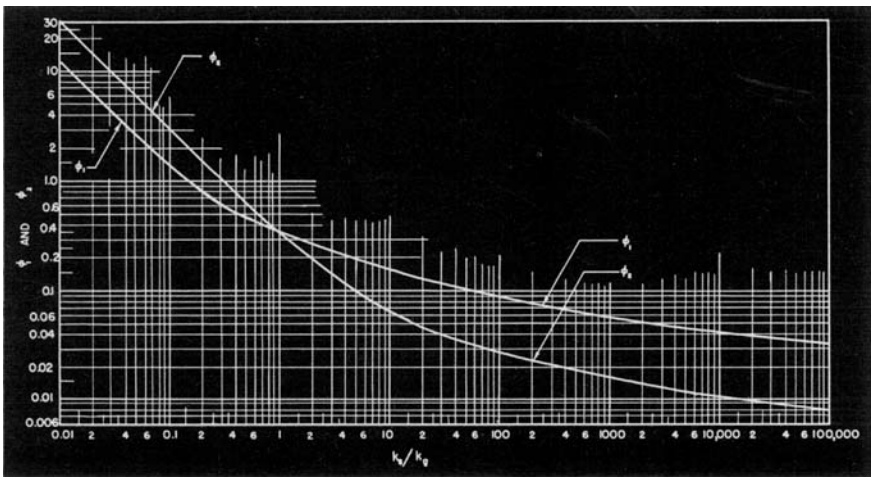

Fig. 5. ϕ vs. thermal-conductivity ratio k_s/k_g; ϕ_1-loose packing, ϕ_2-close packing.

TABLE 2—KEY FOR FIGURE 7

Symbol	Solid	Av. diam. (in.)	Void fraction	Observer	Ref.
⊙	chrome steel sphere	0.15	0.38	Kling	(21)
○	steel sphere	0.157-0.219	0.38-0.394	Waddams	(40)
●	stainless steel sphere	0.0071	0.476-0.502	Preston	(29)
△	SiC	0.00236-0.0216	0.410-0.428	Kannuluick	(19)
◘	diphenyl-amine	0.00106	0.513	Kannuluick	(19)

contact points for all the three orientations will be approximately

$$n_1 = \frac{1}{3}(1 + n' + n'') =$$

$$\frac{1}{3}(1 + 0.945 + 2.31) = 1.42 \sim 1.5$$

As seen in Figure 4, one symmetrical axis is sufficient for the close packing state. The equivalent number of the contact points related to state 1, orientation (a), is

$$n_2 = (6)\frac{D_p^2}{(\sqrt{3}/2)\,D_p^2} = 4\sqrt{3}$$

When one uses these values of n to determine θ_o, Equation (13) can be used to obtain values of ϕ for each packing state. The results plotted vs. the ratio k_s/k_g are shown in Figure 5.

The void fractions for the two cases are

$$\text{State 1: } \epsilon_1 = 1 - \frac{\pi}{6} = 0.476$$

$$\text{State 2: } \epsilon_2 = 1 - \frac{\sqrt{2\pi}}{6} = 0.260$$

It is supposed that actual packed beds may be considered a composite of the two basic packing states. Since ϕ is proportional to the thermal resistance, the correct value for an actual bed should be approximately an additive function of ϕ_1 and ϕ_2. Hence for a bed with a void fraction ϵ, ϕ is given by

$$\phi = \phi_2 + (\phi_1 - \phi_2)\frac{\epsilon - \epsilon_2}{\epsilon_1 - \epsilon_2} = \phi_2 +$$

$$(\phi_1 - \phi_2)\frac{\epsilon - 0.260}{0.216} \text{ for } \epsilon_1 \geqq \epsilon \geqq \epsilon_2 \quad (14)$$

For particles of uniform size it is not possible for the void fraction to be less than ϵ_2. Therefore observed values less than ϵ_2 might be considered the result of clogging by smaller particles in the void spaces. For such cases it seems advisable to use ϵ_2 rather than the extrapolated value from Equation (14). Similarly, observed void fractions larger than ϵ_1 would be caused by the presence of exceptionally large hollow spaces compared with the average void space. This could not contribute significantly to the effective thermal conductivity. Hence for such cases it is proposed that approximately

$$\phi = \phi_1 \text{ for } \epsilon \geq \epsilon_1$$

$$\phi = \phi_2 \text{ for } \epsilon \leq \epsilon_2 \quad (15)$$

COMPARISON WITH EXPERIMENTAL DATA—UNCONSOLIDATED PARTICLES

Equations (8) and (9) were used to predict stagnant conductivities for comparison with the available experimental data. The values of k_s, k_g, D_p, ϵ, and the mean temperature, needed for the calculations, were taken from the published papers. The agreement between computed and observed stagnant conductivities is good, as illustrated graphically in Figures 6 to 8. In Figure 6 are included the systems for which the void fraction is close to 0.42 and the computed curves are based upon this value. Figure 8 includes almost all the published data that have been found for the stagnant conductivity. The ranges of experimental conditions in Figure 8 are as follow:

solids: diphenylamine, naphthalene, coal, calcite, silica, carborundum, steel, lead, copper, aluminum

average particle diameter: from 0.00106 to 0.312 in.

fluid: gas—carbon dioxide, air, nitrogen, methane, propane, helium, hydrogen

liquid—water, glycerine, *iso*-octane, ethyl alcohol, mercury

As previously mentioned, there are available a number of investigations on effective thermal conductivities in packed beds through which fluids are flowing. Although the procedure is somewhat inaccurate, k_s° can be obtained from these data by the extrapolation to zero flow rate. Figure 9 shows the comparison of k_s° values de-

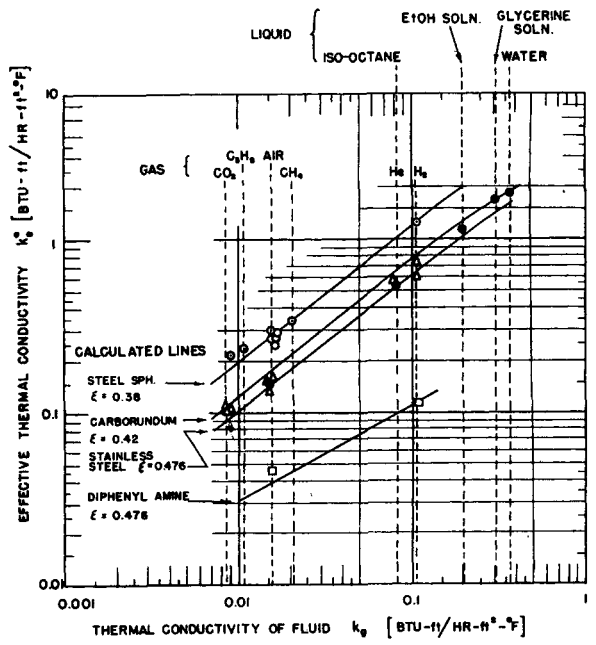

Fig. 7. Comparison of calculated and experimental data, unconsolidated particles.

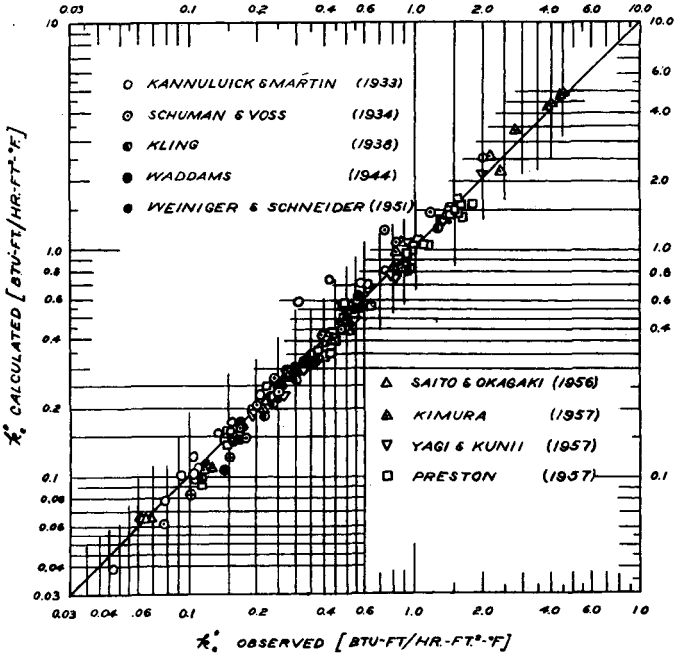

Fig. 8. Comparison of calculated and experimental data for packed beds of unconsolidated particles with motionless fluids.

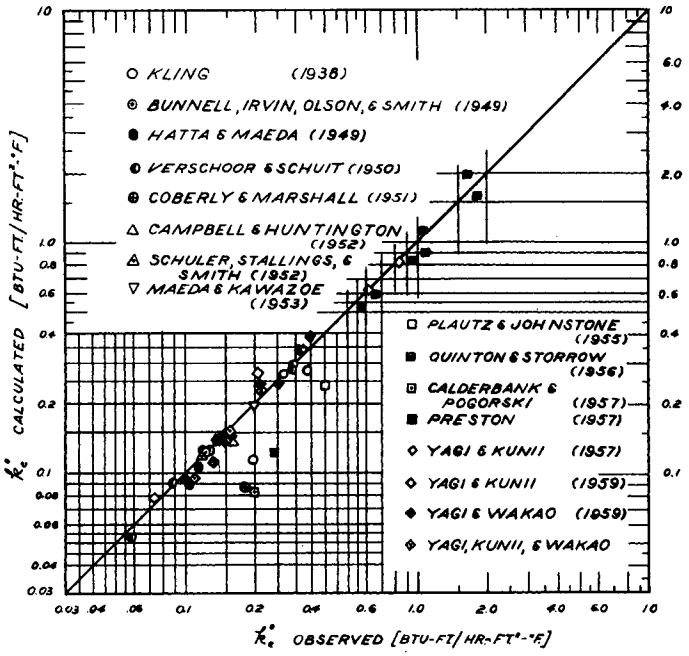

Fig. 9. Comparison of calculated and experimental data obtained by extrapolation of results for moving fluids.

termined in this manner with those computed from Equations (8) and (9). The experimental conditions for the various investigations are as follows:

solids: pumice, terrana, limestone, silica, glass, celite, insulating firebrick, alundum, steel, lead, aluminum

average diameter: from 0.0063 to 0.65 in.; spheres, cylinders, etc.

fluid: gas—air, natural gas
liquid—*iso*-octane, ethyl alcohol, water

Figures 6 to 8 show data for a large range of particle sizes and thermal conductivities of solid and fluid phases. The agreement between the predicted and observed stagnant conductivities suggests that the proposed prediction method may be used with confidence for a variety of beds of unconsolidated particles. The next step is the extension of the theory to consolidated particles.

EXTENSION OF THEORY TO CONSOLIDATED POROUS MEDIA

It has been suggested earlier that at least some kinds of consolidated porous media, for instance sandstone or sintered porous metal, originate as beds of unconsolidated particles. Then consolidation might occur by partial clogging with the cementing substance or by sintering. The original bed of unconsolidated particles is clogged with cementing substance as shown in Figure 10*a*. In this case some parts of the void space would become clogged, and the rest remain open. The result of consolidation is an increase in the average grain size. However the pore size is the same as in the original packed bed.

The mechanism of heat transfer for this model is assumed to be as shown in Figure 10*b*. Here heat is flowing in the vertical direction through the void space, ϵ' and through the solid fraction, $1-\epsilon'$. In this latter part the flow is in series through solid of thickness l'_s and fluid of thickness l_v. The detailed mechanisms of heat transfer are similar to those for unconsolidated particles (Figure 1), except that the shape and relative size of void and solid spaces differ.

Since the average thickness of the fluid film is assumed to be the same for both the original packed bed and the clogged porous media, the number of solid layers in the consolidated bed is proportional to its void fraction and may be written as

$$\frac{N'}{N} = \frac{\epsilon'}{\epsilon} \tag{16}$$

The average length of the unit of clogged solid is inversely proportional to the number of such solid units:

$$\frac{l'_s}{l_s} = \frac{N}{N'} \tag{17}$$

When one uses the detailed mechanisms of heat transfer similar to Figure 1, the resultant expression for k_e° is the same as Equation (6) for unconsolidated particles, except that ϵ and l_s are replaced by ϵ' and l'_s. From Figure 10 it seems reasonable to propose that

$$\Delta L = l'_s + l_v \text{ and } l_s = D_p \tag{18}$$

Combining Equations (17) and (18)

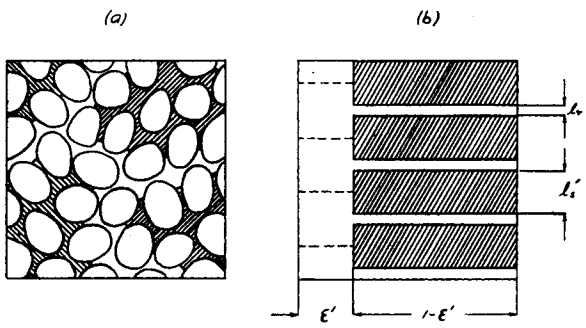

Fig. 10. Model of consolidated porous media.

yields

$$\frac{l'_s}{D_p} = \frac{N}{N'} = \frac{\epsilon}{\epsilon'} \tag{19}$$

The desired expression for k_e° can then be obtained from Equation (6) by first replacing ϵ and l_s with ϵ' and l'_s and then using Equation (18) and (19) for ΔL and l'_s. The result, converted to the form of k_e°/k_s, is

$$\frac{k_e^\circ}{k_s} = \epsilon'\frac{k_g}{k_s} + \epsilon\frac{D_p h_{rv}}{k_s}\left(1+\frac{\epsilon'}{\epsilon}\phi\right) + \frac{(1-\epsilon')\left(1+\frac{\epsilon'}{\epsilon}\phi\right)}{1+\frac{(\epsilon'/\epsilon)}{\frac{1}{\phi}\left(\frac{k_g}{k_s}\right)+\frac{D_p(h_p+h_{rs})}{k_s}}} \tag{20}$$

Equation (20) includes the term involving h_p, since this mechanism may be important in consolidated beds.

For most temperatures the radiation terms are negligible, and Equation (20) reduces to

$$\frac{k_e^\circ}{k_s} = \epsilon'\left(\frac{k_g}{k_s}\right) + \frac{(1-\epsilon')\left(1+\frac{\epsilon'}{\epsilon}\phi\right)}{1+\frac{(\epsilon'/\epsilon)}{\left(\frac{1}{\phi}\right)\frac{k_g}{k_s}+\frac{D_p h_p}{k_s}}} \tag{21}$$

The heat transfer through the contact surface between consolidated particles, represented by the dimensionless group $h_p D_p/k_s$ in Equation (21), cannot be easily evaluated. It is characteristic of the kind of solid material and the type of consolidation. It will be regarded as a consolidation parameter to be determined by comparing experimental data with Equation (21).

COMPARISON WITH EXPERIMENTAL DATA—CONSOLIDATED PARTICLES

To treat porous media over a relatively large range of void fraction, namely 0 to 0.40, state 1 is chosen as the basic fundamental packing arrangement for consolidated particles.

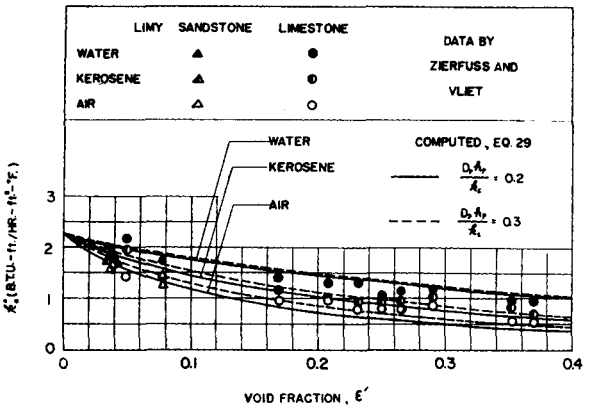

Fig. 11. Comparison of stagnant conductivities for limestone.

Then the required ϕ value can be obtained from the line of ϕ_1, in Figure 5, and $\bullet$ taken as 0.476, both for use in Equation (21). The consolidation parameter $D_p h_p/k_s$ is independent of the fluid in the pores of the void fraction.

Figure 11 shows the comparison of calculated lines with the experimental data for different fluids in limestone and limy sandstones originating in different places, that is the Netherlands, France, and California. When one assumes $D_p h_p/k_s$ as 0.2 and 0.3 in Equation (21), the calculated lines explain reasonably well the variation of k_e^o with void fraction. These computed results are based upon a value of k_s = 2.24 B.t.u./(hr.)-(ft.)(°F), as taken from the International Critical Tables.

The experimental data for sandstones by Zierfuss and Vliet (*50*), Clark (*7*), and Asaad (*2*) are compared with calculated results in Figure 12. Since the thermal conductivity of the solid phase is the mean value of the clogged group of particles, as shown in Figure 10*a*, the numerical value of k_s is not necessarily the same as that of pure quartz but rather may lie between the values of quartz and of the cementing material. In view of this, three different values of k_s, 5, 4, and 3, were used in Equation (21). Hence in Figure 12 three computed curves are shown. The consolidation parameter was taken as 0.2 for all three computed curves. It should be noted that samples from the same country originated in nearly every case from two or three different formations. Hence the consolidation parameter and thermal conductivities of the clogged material probably were different not only from country to country but for different samples from the same country. As in Figure 11, the variation of stagnant conductivity with void fraction is predicted well by Equation (21), although the absolute experimental values scatter. This suggests that the proposed theory correctly reflects the effect of void fraction. In addition, the data in Figures 11 and 12 indicate that the influence of the thermal conductivity of the fluid is adequate accounted for.

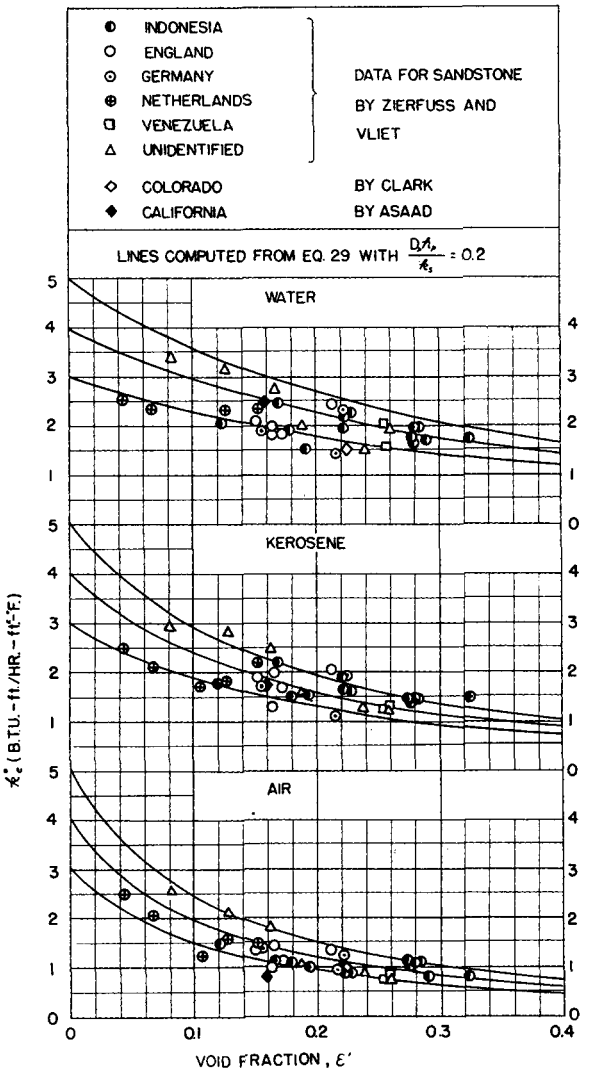

Fig. 12. Comparison of stagnant conductivities for sandstone.

Saunders *et al.* (*15*) presented the experimental data for effective thermal conductivities of sintered porous metals within stagnant air. Since the composition of the metal, a copper-tin alloy, was not given, the arithmetic mean value of the thermal conductivity taken as k_s = 120 B.t.u.-ft./(hr.)(sq.ft.)-(°F.) was employed. When one assumes the dimensional group $D_p h_p/k_s$ to be 0.075, the calculated line agrees well with the experimental data, as shown in Figure 13.

CONCLUSIONS

Equations (7) to (9) appear to predict with reasonable accuracy the effective thermal conductivities for various types of beds of unconsolidated particles filled with stationary fluid. The development is based upon proposing a model for the various mechanisms of heat transfer. The data required for using Equations (7) to (9) are the thermal conductivities of the solid and fluid phases and the void fractions of the bed. If radiation contributions are significant, other information is needed.

The theory was extended to beds of consolidated particles such as sandstone and sintered-metal particles. A dimensionless consolidation parameter was introduced to account for the heat

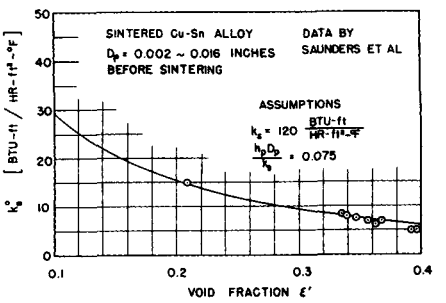

Fig. 13. Comparison of calculated and experimental data for sintered porous copper-tin alloy.

transfer through the contact surfaces of the consolidated particles. This parameter is a specific property of the consolidation state and the solid phase. Values of 0.2 to 0.3 satisfactorily explained available data for sandstone, but smaller values were necessary for sintered metal particles, reflecting the larger thermal conductivity of the metallic solid phase. The theoretical development satisfactorily correlated data for a variety of fluid and solid materials over a range of void fraction.

In future work it is planned to extend the same method of approach to consolidated beds filled with moving fluid.

ACKNOWLEDGMENT

The authors wish to express their appreciation to The Technological Institute, Northwestern University, for its financial assistance in carrying on this study.

NOTATION

D_p = diameter of unconsolidated particles in a packed bed or diameter of original particles before clogging in consolidated porous media, ft.

h_p = heat transfer coefficient representing the heat transfer rate through the contact surface between solid particles in a bed of unconsolidated particles or between two clogged particles in a consolidated bed, B.t.u./(hr.)-(sq.ft.)(°F.)

h_{rs} = heat transfer coefficient for thermal radiation, solid surface to solid surface, B.t.u./-(hr.)(sq.ft.)(°F.)

h_{rv} = heat transfer coefficient for thermal radiation, void space to void space, B.t.u./(hr.)-(sq.ft.)(°F.)

k_e^o = stagnant conductivity, that is effective thermal conductivity of porous media filled with stagnant fluid for both unconsolidated and consolidated particles, (B.t.u.)-(ft.)/(hr.)(sq.ft.)(°F.)

k_g = thermal conductivity of fluid, (B.t.u.)(ft.)/(hr.)(sq.ft.)-(°F.)

k_s = thermal conductivity of solid phase, (B.t.u.)(ft.)/(hr.)-(sq.ft.)(°F.)

ΔL = effective length between centers of two neighboring solid particles in direction of heat flow, ft.

l_s = effective length of a solid particle for heat transfer in a bed of unconsolidated particles, ft.

l_s' = effective length of a clogged particle for heat transfer in a bed of consolidated particles, ft.

l_v = effective thickness of the fluid film adjacent to the surface of two solid particles, ft.

N = number of solid particles in a unit length of packed bed, measured in the direction of heat flow

N' = number of clogged particles in a unit length of consolidated porous media, measured in the direction of heat flow

n = number of contact points on a semispherical surface of one solid particle

q = heat flow rate, B.t.u./hr.

q_s = heat flux through solid phase, B.t.u./hr.-sq.ft.

R = radius of solid particle, ft.

t = temperature, °F.

Δt = increment of temperature, °F.

x_0 = diameter of sectional area corresponding to one contact point, ft.

Greek Letters

β = $\Delta L/D_p$

γ = l_s/D_p

ϕ = l_v/D_p

ϕ_1 = ϕ value corresponding to the loose or most open packing of spheres

ϕ_2 = ϕ value corresponding to the closest packing of spheres

κ = k_s/k_g

ϵ = void fraction of a packed bed of unconsolidated particles

ϵ_1 = void fraction corresponding to the most open packing arrangement

ϵ_2 = void fraction corresponding to the closest packing arrangement

ϵ' = void fraction of a bed of consolidated porous media

θ = angle, radians

θ_0 = angle corresponding to boundary of heat flow area for one contact point, radians

LITERATURE CITED

1. Argo, W. B., and J. M. Smith, *Chem. Eng. Progr.*, **49**, 1977 (1953).
2. Asaad, T., Ph. D. thesis, Univ. Calif., Berkeley (June, 1955).
3. Birch, F., and H. Clark, *Am. J. Sci.*, **238**, 529 (1940).
4. Bunnell, D. G., H. B. Irvin, R. W. Olson, and J. M. Smith, *Ind. Eng. Chem.*, **41**, 1977 (1949).
5. Calderbank, P. H., and L. A. Pogorski, *Trans. Inst. Chem. Engrs. (London)*, **35**, 195 (1957).
6. Campbell, J. M., and R. L. Huntington, *Petrol. Refiner*, **31**, 123 (1952).
7. Clark, H., *Trans. Am. Geophys. Union*, 543 (1941).
8. Clyde, O., Jr., *Ind. Eng. Chem.*, **47**, 356 (1955).
9. Coberly, C. A., and W. R. Marshall, Jr., *Chem. Eng. Progr.*, **47**, 141 (1951).
10. Eucken, A., *Forsch. Gebiete Ingenieurw.*, **133**, *Forschungsheft*, No. 353, 16 (1932).
11. Felix, J. R., and W. K. Neil, unpublished paper.
12. Francl, J., and W. D. Kingery, *J. Am. Ceram. Soc.*, **37**, 99 (1954).
13. Gemant, A., *J. Appl. Phys.*, **21**, 750 (1950).
14. Gore, D. E., and B. J. Fulker, *Status Rep. Am. Petrol. Inst.* (Aug. 1, 1957 to July 31, 1958).
15. Grootenhuis, D., R. C. A. Mackworth, and U. A. Saunder, *Inst. Mech. Engrs. (London)*, 363 (1951).
16. Harbert, W. D., D. C. Cain, and R. L. Huntington, *Ind. Eng. Chem.*, **33**, 257 (1949).
17. Hatta, S., and S. Maeda, *Chem. Eng. (Japan)*, **12**, 56 (1948); **13**, 79 (1949).
18. Hougen, J. O., and E. L. Piret, *Chem. Eng. Progr.*, **47**, 287 (1951).
19. Kannuluick, W. G., and L. H. Martin, *Proc. Roy. Soc. (London)*, **A141**, 144 (1933).
20. Kimura, M., *Chem. Eng. (Japan)*, **21**, 472 (1957).
21. Kling, G., *Forsch. Gebiete Ingenieurw.*, **9**, 28, 82 (1938).
22. Kwong, S. S., and J. M. Smith, *Ind. Eng. Chem.*, **49**, 894 (1954).
23. Loeb, A. L., *J. Am. Ceram. Soc.*, **37**, 96 (1954).
24. Maeda, S., and K. Kawazoe, *Chem. Eng. (Japan)*, **15**, 5, 9, 312 (1951); **17**, 276 (1953); **18**, 279 (1954).
25. Morales, M., C. W. Spinn, and J. M. Smith, *Ind. Eng. Chem.*, **43**, 226 (1951).
26. Molino, D. F., and J. O. Hougen, *Chem. Eng. Progr.*, **48**, 147 (1952).
27. Niven, C. D., *Can. J. Research*, **18**, 132 (1940).
28. Plautz, D. A., and H. F. Johnstone, *A.I.Ch.E. Journal*, **1**, 193 (1955).
29. Preston, F. W., Ph.D. thesis, Penn. State Univ., State College (June, 1957).
30. Quinton, J. H., and J. A. Storrow, *Chem. Eng. Sci.*, **5**, 245 (1956).
31. Ranz, W. E., *Chem. Eng. Progr.*, **48**, 247 (1952).
32. Russell, H. W., *J. Am. Ceram. Soc.*, **18**, 1 (1954).
33. Saito, T., and O. Okagaki, *Bull. Fac. Eng., Hokkaido Univ.*, No. 14, 83 (1956).
34. Schneider, W. G., *Ind. Eng. Chem.*, **46**, 828 (1954).
35. Schuler, R. W., V. P. Stallings, and J. M. Smith, *Chem. Eng. Progr. Symposium Ser. No. 4*, **48** (1952).
36. Schumann, T. E. W., and V. Voss, *Fuel*, **13**, 249 (1934).
37. Singer, E., and R. H. Wilhelm, *Chem. Eng. Progr.*, **46**, 343 (1950).
38. Stricker, H. S., *J. Chem. Phys.*, **20**, 1333 (1952).
39. Verschoor, H., and G. Schuit, *Appl. Sci. Research*, **42**, A297 (1950).
40. Waddams, A. L., *J. Soc. Chem. Ind.*,

63, 337 (1944); *Chem. & Ind. (London)*, 206 (1944).
41. Webb, J., *Nature*, **177**, 989 (1956).
42. Weiniger, J. L., and W. G. Schneider, *Ind. Eng. Chem.*, **43**, 1229 (1951).
43. Wilhelm, R. H., W. C. Wynkoop, and D. W. Collier, *Chem. Eng. Progr.*, **44**, 105 (1948).
44. Woodside, W., *Can. J. Phys.*, **36**, 815 (1958).
45. Yagi, Sakae, and Daizo Kunii, *Chem. Eng. (Japan)*, **18**, 576 (1954); *A.I.Ch.E. Journal*, 3, 373 (1957).
46. ———, *A.I.Ch.E. Journal*, to be published.
47. ———, and Y. Shimoura, *Chem. Eng. (Japan)*, **21**, 342 (1952.
48. ———, and N. Wakao, *A.I.Ch.E. Journal*, to be published.
49. Yagi, S., and N. Wakao, *A.I.Ch.E. Journal*, **5**, 79 (1959).
50. Zierfuss, H., and G. Vliet, *Bull. Am. Assoc. Petrol. Geologists*, **40**, No. 10, 2475 (1958).

Manuscript received June 5, 1959; revision received July 17, 1959; paper accepted August 3, 1959. Paper presented at A.I.Ch.E. San Francisco meeting.

Hypothetical Standard States and the Thermodynamics of High-Pressure Phase Equilibria

J. M. PRAUSNITZ

University of California, Berkeley, California

Thermodynamic analysis of phase-equilibrium data is necessary for testing such data, for extension to new conditions, and for purposes of correlation and prediction of phase-equilibrium behavior. While such analysis is common for low-pressure systems, it is rare for high-pressure systems owing to difficulties encountered in the definition of standard states. For a gaseous solute in the liquid phase it is proposed that the standard state be taken as the hypothetical liquid at the temperature and total pressure of the solution. The properties of this standard state are specified by the temperature and total pressure and by the specific volume which the substance would have if it did not experience a phase change. This standard state is useful since it is not a function of the solution but only of the substance being considered. For a condensable component in the gas phase it is convenient for most purposes to define the standard state as the ideal gas at the temperature and total pressure of the solution, but to separate the effect of composition on the activity coefficient from that of pressure, it is proposed to define the standard state as the real hypothetical gas at the solution conditions. To illustrate these ideas, activity coefficients are computed for several high-pressure systems, and it is shown how these activity coefficients may be used in the correlation, testing, and extension of high-pressure phase-equilibrium data.

Thermodynamic analysis of phase-equilibrium data is needed for testing and correlating such data and especially for extension to new conditions and to other systems for which no data are available. It is not reasonable to expect that good data for a very large number of systems will ever be obtained over wide ranges of temperature and pressure, and it is therefore essential that available data for representative systems be carefully scrutinized and interpreted with the aid of suitable thermodynamic functions. Such thermodynamic analysis, coupled with the theory of intermolecular forces and aided by techniques like the molecular theory of corresponding states, forms the basis for a useful generalization of phase-equilibrium data. The primary justification for thermodynamic analysis is that it is the first important step toward the ultimate aim of solution theory: prediction of the properties of a mixture from those of the pure components.

In the technical literature it has been customary to subject to thermodynamic analysis equilibrium data for solutions taken at or near atmospheric pressure, but there has been a notable absence of such analyses for phase-equilibrium data obtained at higher pressures in the vicinity of 100 atm. or more. For example some of the excellent experimental studies of Sage and Lacey and W. B. Kay and their co-workers on hydrocarbon mixtures have been in the literature for many years but have received very little thermodynamic scrutiny. A major reason for the lack of thermodynamic attention to high-pressure systems is that when the customary thermodynamic functions of the high-pressure mixture are referred to those of the pure components, these components exist in physically unattainable (hypothetical) states. Thermodynamic analysis of high-pressure systems therefore requires precise definitions of hypothetical standard states as well as methods of evaluating the thermodynamic functions corresponding to those states. This paper presents techniques for the calculation of hypothetical standard-state functions and in a few examples illustrates their applicability to thermodynamic analysis of high-pressure phase equilibria.

STANDARD STATES

The activity coefficient of a compo-